Liquid Crystals
Publication details, including instructions for authors and subscription information:
http://www.informaworld.com/smpp/title~content=t713926090

Molecular dynamics simulations of discotic liquid crystals using a hybrid Gay-Berne Luckhurst-Romano potential

M. D. De Luca[ab]; M. P. Neal[abc]; C. M. Care[ad]
[a] Sheffield Hallam University, Sheffield, England [b] Division of Applied Physics, [c] School of Mathematics and Computing, University of Derby, Derby [d] Materials Research Institute,

To cite this Article De Luca, M. D. , Neal, M. P. and Care, C. M.(1994) 'Molecular dynamics simulations of discotic liquid crystals using a hybrid Gay-Berne Luckhurst-Romano potential', Liquid Crystals, 16: 2, 257 — 266
To link to this Article: DOI: 10.1080/02678299408029150
URL: http://dx.doi.org/10.1080/02678299408029150

LIQUID CRYSTALS, 1994, VOL. 16, NO. 2, 257–266

Molecular dynamics simulations of discotic liquid crystals using a hybrid Gay–Berne Luckhurst–Romano potential

by M. D. DE LUCA†, M. P. NEAL*†‡ and C. M. CARE§
Sheffield Hallam University, City Campus,
Pond Street, Sheffield S1 1WB, England

(*Received 5 April 1993; accepted 12 July 1993*)

We report the results of the computer simulation of a collection of particles interacting via an anisotropic potential proposed by Luckhurst and Romano and modified by scaling with part of the anisotropic well depth formalism employed by Gay–Berne. Using the molecular dynamics technique for 256 particles in the NVE ensemble, the system is shown to exhibit a variety of mesophases, as the temperature is lowered, and these are provisionally identified as isotropic, discotic nematic, a highly ordered fluid phase with some columnar features and a crystal.

1. Introduction

Significant progress has been made in recent years in modelling liquid crystal phases using hard non-spherical models, soft non-spherical models and realistic atom–atom potentials. Orientationally ordered mesophases have been simulated using non-spherical rod-like and disc-like hard-core mesogens [1–3], but longer range attractive forces are expected to influence the formation of mesophases, as well as short range repulsive forces. Luckhurst and Romano [4] represented cylindrically symmetric particles by a Lennard–Jones 12–6 potential, V_0 together with an additional anisotropic term V_a

$$V = V_0 + V_a, \tag{1}$$

where

$$V_0 = 4\varepsilon\left\{\left(\frac{\sigma}{r}\right)^{12} - \left(\frac{\sigma}{r}\right)^{6}\right\}, \tag{2}$$

$$V_a = -4\lambda\varepsilon\left\{\left(\frac{\sigma}{r}\right)^{12} + \left(\frac{\sigma}{r}\right)^{6}\right\}P_2(\cos(\beta_{12})) \tag{3}$$

and β_{12} is the angle between the particle symmetry axes. They demonstrated a weak first order transition from a nematic to an isotropic phase using a value of $\lambda = 0{\cdot}15$ determined by preliminary calculations.

Everitt and Care [5] carried out a Monte Carlo simulation of a siloxane ring system using the Luckhurst and Romano potential given by equation (1) to represent the mesogenic units attached to the ring. The system exhibited a transition from calamitic ordering to discotic ordering as the ring–mesogen bond varied from fully rigid to fully flexible.

---

* Author for correspondence.

† Division of Applied Physics.

‡ Present address, School of Mathematics and Computing, University of Derby, Derby DE22 1GB.

§ Materials Research Institute.

Berne and Pechukas [6] developed a soft non-spherical single site potential based on the Gaussian overlap model. The original potential had several unrealistic features and was modified [7] by obtaining a function which gave the best fit to the potential described by a linear array of four equidistant Lennard–Jones centres. This potential has been used extensively by Luckhurst and co-workers, for example, [8, 9] and by de Miguel and Rull [10] with rod-like parameterization to simulate nematic, smectic A and smectic B phases, and by Emerson and Luckhurst [11] with disc-like parameterization to simulate discotic nematic and discotic columnar phases. The Gay–Berne potential is a single site potential so that a smooth transition in shape is obtained as the parameterization is varied from the rod-like to the disc-like form. To model the complex spectrum of molecular interactions of rods and discs more realistically, we propose in future work to rigidly join together soft anisotropic potentials in a variety of geometries. Such simulations are computationally very expensive, so in a bid to reduce the time required, we have investigated a modified form of potential (1) [12]. The pair potential is scaled by part of the well depth formalism employed to fit the Gay–Berne potential [7], where

$$\varepsilon'(\hat{\mathbf{u}}_1, \hat{\mathbf{u}}_2, \mathbf{r}) = 1 - \frac{\chi'}{2}\left\{\frac{(\hat{\mathbf{r}}\cdot\hat{\mathbf{u}}_1 + \hat{\mathbf{r}}\cdot\hat{\mathbf{u}}_2)^2}{1+\chi'(\hat{\mathbf{u}}_1\cdot\hat{\mathbf{u}}_2)} + \frac{(\hat{\mathbf{r}}\cdot\hat{\mathbf{u}}_1 - \hat{\mathbf{r}}\cdot\hat{\mathbf{u}}_2)^2}{1-\chi'(\hat{\mathbf{u}}_1\cdot\hat{\mathbf{u}}_2)}\right\} \tag{4}$$

so that the potential becomes

$$V = \varepsilon'(\hat{\mathbf{u}}_1, \hat{\mathbf{u}}_2, \mathbf{r})\{V_o + V_a\}. \tag{5}$$

The orientation of the molecule is specified by the unit vector $\hat{\mathbf{u}}$ and the intermolecular vector by the unit vector $\hat{\mathbf{r}}$. The parameter χ' determines the relative ratio of the end to end and side to side interactions and is given by

$$\chi' = (1 - \varepsilon_e/\varepsilon_s)/(1 + \varepsilon_e/\varepsilon_s), \tag{6}$$

where $\varepsilon_e/\varepsilon_s$ is the ratio of end to end and side to side potential well depths [8]. The original potential (1) is dependent on the relative orientation of the intermolecular axes and so favours end to end (e) and side to side (s) configurations compared to cross (X) and tee (T) configurations, but does not distinguish between side–side and end–end or between X and T. It should be noted however that the modified potential given by equation (5) does distinguish between s and e and between X and T, as shown in table 1. The modified potential (5) requires one tenth the CPU time of the Gay–Berne on an iPSC860 processor. Further it has the advantage that the effect of ε' alone can be investigated by varying $\varepsilon_e/\varepsilon_s$. Extensive studies of the Gay–Berne fluid have used values of 5·0 to represent a disc-like potential and 0·2 or less [11] to represent a rod-like potential as part of the parameterization. Setting the ratio equal to 1 removes the effect of ε'. We present preliminary results for potential (5) with $\lambda = 0{\cdot}15$ and $\varepsilon_e/\varepsilon_s$ equal to 5·0 so that the end to end interaction is favoured as shown in figure 1.

Table 1. Values of $\varepsilon'(\hat{\mathbf{u}}_1, \hat{\mathbf{u}}_2, \mathbf{r})$ (4), for different configurations.

Configuration	$\varepsilon_e/\varepsilon_s = 0{\cdot}2$	$\varepsilon_e/\varepsilon_s = 5{\cdot}0$	β_{12}	$\varepsilon'(\hat{\mathbf{u}}_1, \hat{\mathbf{u}}_2, \mathbf{r})$
end–end	0·2	5·0	0°	$\varepsilon_e/\varepsilon_s$
side–side	1·0	1·0	0°	1
X	1·0	1·0	90°	1
T	1·0/3·0	5·0/3·0	90°	$2/(1+\varepsilon_s/\varepsilon_e)$

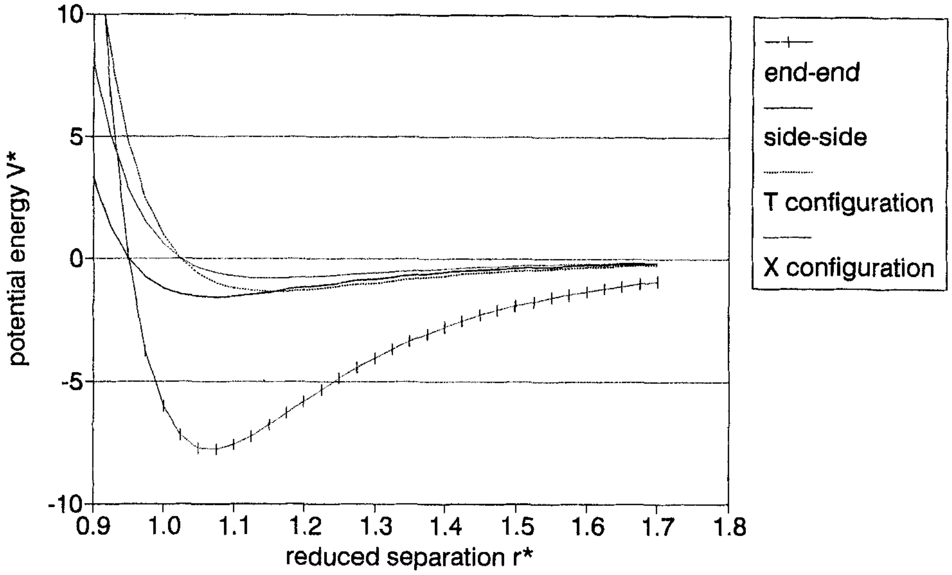

Figure 1. The distance dependence of the potential energy calculated from the modified anisotropic potential for particular orientations of the molecules with respect to one another and to the intermolecular vector. The parameterization of the potential is that used in the molecular dynamics simulation and described in the text.

2. Molecular dynamics simulation

Our primary aim was to see if potential (5) could be used to model discotic liquid crystals, and to compare the phase temperatures with those obtained for the Gay–Berne fluid. We have performed molecular dynamics simulations (MD) for 256 particles in the NVE ensemble in a cubic box, employing periodic boundary conditions. No cut off was used as this did not aid the vectorization, and one time step in the simulation required 0·03 s of CPU time on an Amdahl VP1200 supercomputer. The translational equations of motion were solved numerically using a Verlet half-step leapfrog algorithm [13, 14], and the rotational equations of motion were solved in a similar manner using a constraint method [15]. Preliminary calculations were performed with a variety of number densities and at low temperatures. At values close to that of liquid argon near the triple point, cavities formed in the box. Results are presented for a reduced number density $\rho^*=1{\cdot}1$ which enabled equilibration of the system at low temperatures without cavity formation. The particles are axially symmetric about the vector $\hat{\mathbf{u}}$ with a spherical repulsive core surrounded by a non-spherical attractive region, equivalent to a disc-like moment of inertia. A reduced moment of inertia of $I^*=1{\cdot}00$ ($I^*=I/(m\sigma^2)$) was employed to provide a reasonable rate of equilibration between translational and rotational energy. From the simulation, the following quantities were calculated: the pressure $P^*=P\sigma^3/\varepsilon$, temperature $T^*=Tk_B/\varepsilon$, the root mean square displacement $\langle|\mathbf{r}^*(t)-\mathbf{r}^*(0)|^2\rangle^{1/2}$ and its components parallel and perpendicular to the director, the total internal energy per particle $E^*=E/\varepsilon$, the potential and the kinetic energy per particle U^* and K^*, the order parameter $\langle P_2\rangle$ and the director of the phase $\hat{\mathbf{n}}$. The second rank order parameter $\langle P_2\rangle$ was evaluated using the tensor Q defined by

$$Q_{\alpha\beta}=\frac{1}{N}\sum_{i=1}^{N}\frac{3u_\alpha^i u_\beta^i-\delta_{\alpha\beta}}{2}, \qquad (7)$$

where u_α^i is the α-component of the unit vector along the symmetry axis of the molecule i. $\langle P_2 \rangle$ was defined as the ensemble average of the largest eigenvalue of the Q-tensor, and the director as the corresponding eigenvector [16] and these were calculated every 100 steps. Additionally the second rank orientational correlation function G_2,

$$G_2 = \langle P_2(\cos \beta_{ij}(r^*)) \rangle \tag{8}$$

the radial distribution function $g(r)$ together with the longitudinal and transverse pair correlation functions $g_{\parallel}(r_{\parallel}^*)$ and $g_{\perp}(r_{\perp}^*)$ were calculated.

The first simulation was started from an α-fcc crystal with kinetic and rotational energy such that the initial lattice melted. The system was allowed to equilibrate over 30 000 steps, equipartition between translational and rotational energy being observed, and production runs of 30 000 step were employed. The temperature was reduced by scaling the linear velocities and allowing the system to equilibrate for 30 000 steps between each production run. The reduced time step $\Delta t^* = (\varepsilon/m\sigma^2)^{1/2}\Delta t$ was adjusted to give acceptable energy conservation for each state point; fluctuations of less than 1 part in 1000 of the total energy were observed for all runs except one just before the region identified as the isotropic–nematic transition in which the energy fluctuated by 1 part in 100. A valued of $\Delta t^* = 0{\cdot}005$ was employed in the isotropic region, but this was lowered to 0·0015 in regions where the second rank order parameter $\langle P_2 \rangle$ rose indicating the onset of order.

3. Results

The variation of $\langle P_2 \rangle$ as the system was cooled is shown in figure 2. We see that the system is isotropic at a reduced temperature of $\langle T^* \rangle = 10{\cdot}0$ and remains orientationally disordered until the temperature is lowered to about $\langle T^* \rangle = 5{\cdot}5$, although finite size fluctuations in evaluating Q lead to a small non-zero value for $\langle P_2 \rangle$. In the reduced temperature range of $\langle T^* \rangle = 5{\cdot}5$ to $\langle T^* \rangle = 5{\cdot}0$, the order parameter rapidly rises to about $\langle P_2 \rangle = 0{\cdot}64$. It then slowly tends to 1·0 as the system is cooled further. Figure 3

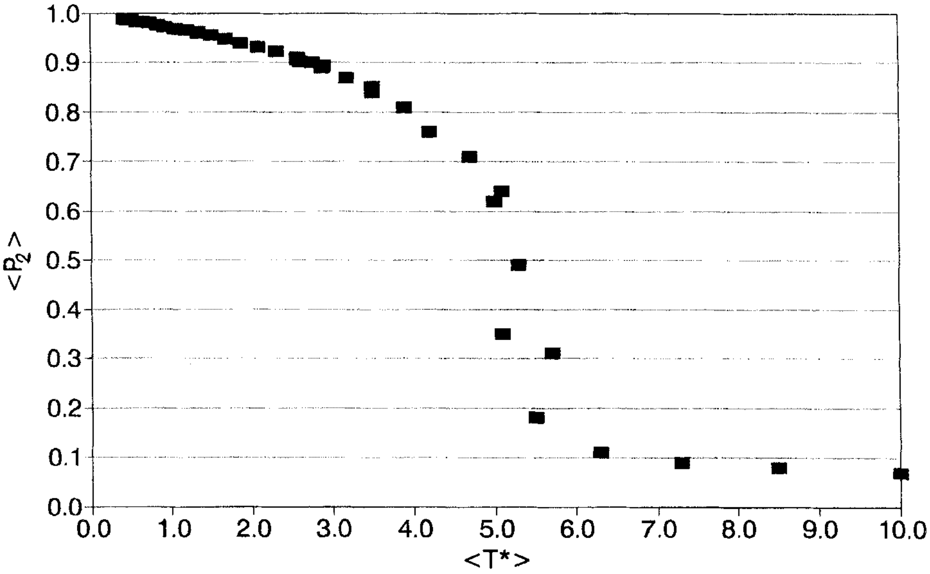

Figure 2. The variation of the second rank orientational order parameter $\langle P_2 \rangle$ as a function of reduced temperature.

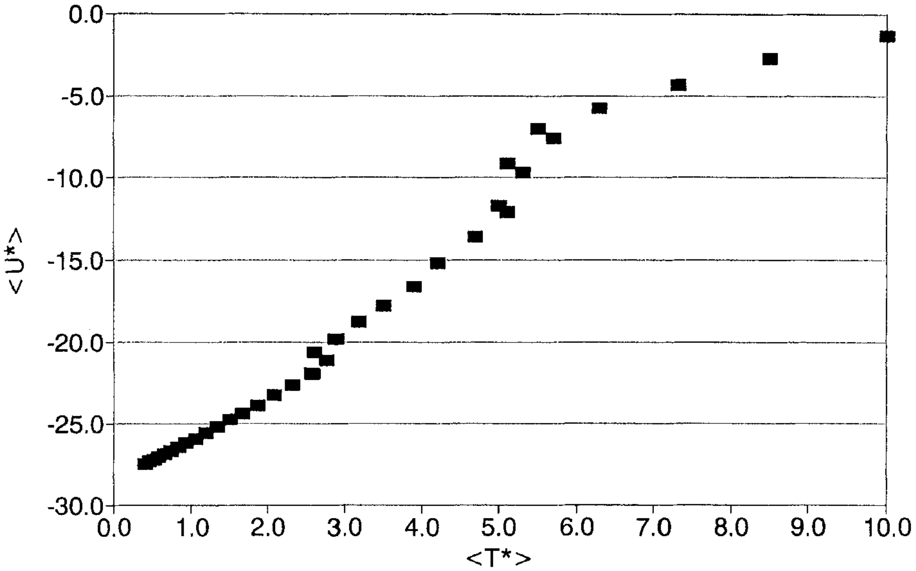

Figure 3. The variation of the potential energy $\langle U^* \rangle$ as a function of reduced temperature.

shows the change of the potential energy with temperature. At reduced temperatures of $5 \cdot 3 \pm 0 \cdot 2$ and $2 \cdot 7 \pm 0 \cdot 1$, a fall in potential energy is seen while the temperature remains constant, indicating the presence of two phase transitions. The entropy of transition $\Delta\langle U^* \rangle / \langle T^* \rangle$ was estimated to be 0·6 in each case. The mean square displacement was monitored during each production run and the diffusion coefficient calculated from its gradient with respect to time as a check on the fluidity of the phase. Simulation runs near phase transitions were extended a further 150 000 steps and the diffusion coefficients D^* and its components $D^*_{\parallel}$ and $D^*_{\perp}$ parallel and perpendicular to the director obtained from the gradient of these curves which relate to the Einstein relation [17], valid at long times, were calculated by considering the final two-thirds of the simulation only. These results are presented in table 2. In these extended runs it was found that close to the nematic–isotropic transition, the system was subject to large energy fluctuations. This problem was resolved by substituting a full step Verlet algorithm to solve the rotational equations of motion [9].

Figure 4(*a*) shows that diffusion in a direction parallel and perpendicular to the director is equal at a reduced temperature of $\langle T^* \rangle = 5 \cdot 0$. This is not observed in simulations of a Gay–Berne discotic nematic fluid [11]. This effect is attributed to the fact that the modified potential has a spherical repulsive core, whereas the repulsive

Table 2. Reduced diffusion coefficients, mean order parameters and mean temperatures.

$\langle T^* \rangle$	D^*	$D^*_{\parallel}$	$D^*_{\perp}$	$\langle P_2 \rangle$
5·3 ± 0·2	57·8	19·4	19·2	0·49 ± 0·06
5·0 ± 0·2	51·7	17·9	16·9	0·62 ± 0·02
2·88 ± 0·08	19·3	6·2	6·6	0·889 ± 0·008
2·77 ± 0·09	5·4	1·3	2·0	0·901 ± 0·007
2·58 ± 0·07	0·7	0·1	0·3	0·911 ± 0·007

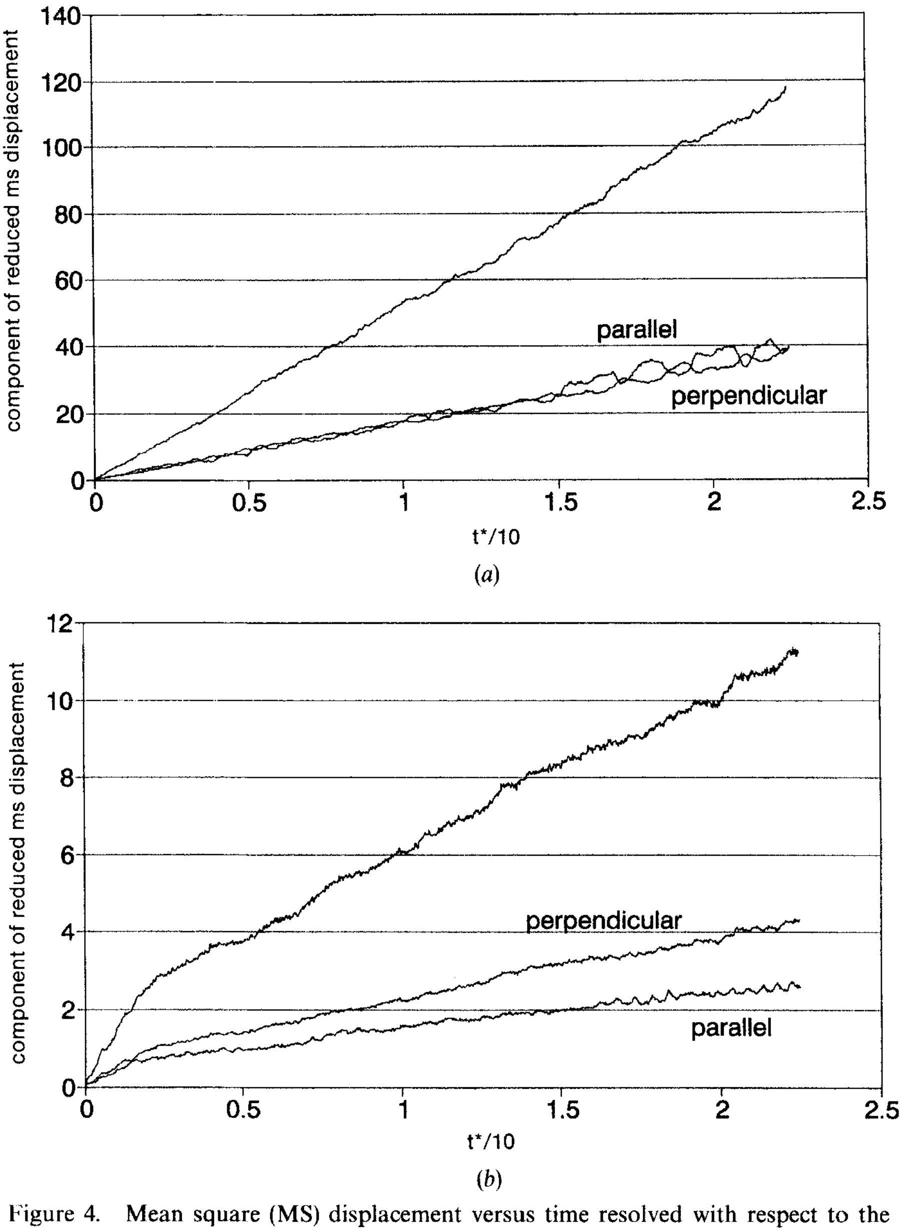

(*a*)

(*b*)

Figure 4. Mean square (MS) displacement versus time resolved with respect to the system director at a reduced temperature of (*a*) $\langle T^* \rangle = 5{\cdot}0$ and (*b*) $\langle T^* \rangle = 2{\cdot}77$.

core of the Gay–Berne potential possesses ellipsoidal symmetry. By the time the system has cooled to a reduced temperature of $\langle T^* \rangle = 2{\cdot}77$, initially coincident curves, describing the components of diffusion with respect to the director, diverge at long time, although the total mean square displacement still exhibits liquid like behaviour, see figure 4(*b*). This reduction in diffusion parallel to the director below $\langle T^* \rangle = 2{\cdot}8$ is further evidence for a transition to a highly ordered, possibly columnar fluid phase. At reduced temperatures lower than $\langle T^* \rangle \approx 2{\cdot}6$, diffusion in all directions has virtually ceased, indicating the presence of a solid like phase.

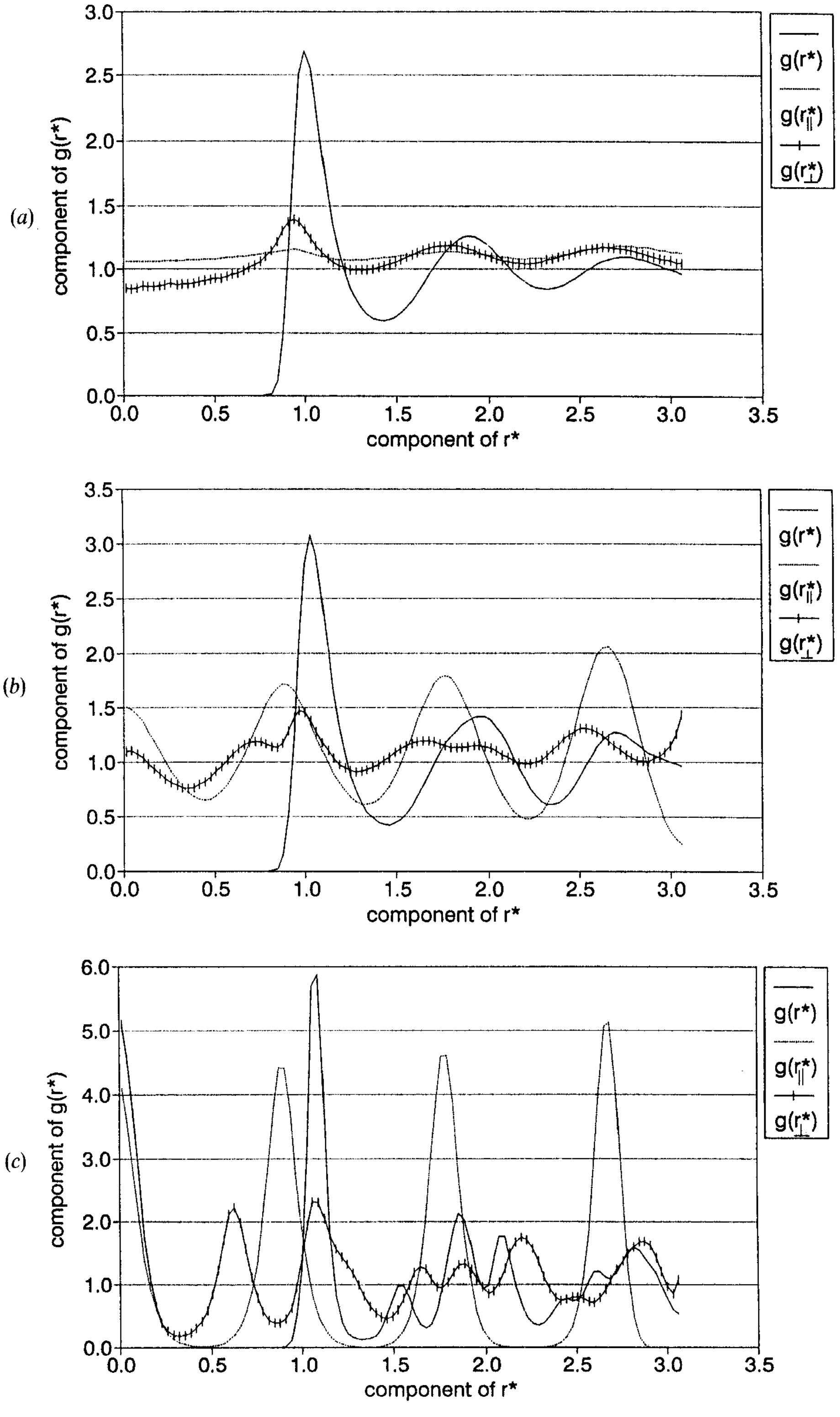

Figure 5. The radial distribution function $g(r^*)$ as a function of the scaled separation r^* and the longitudinal and transverse pair correlation functions $g_{\parallel}(r^*)$ and $g_{\perp}(r^*)$ resolved with respect to the system director as a function of the components of the scaled separations $r_{\parallel}^*$ and $r_{\perp}^*$ respectively, simulated for the modified anisotropic potential at a series of reduced temperatures (*a*) $\langle T^* \rangle = 5{\cdot}0$, $\langle P_2 \rangle = 0{\cdot}62$, (*b*) $\langle T^* \rangle = 2{\cdot}77$, $\langle P_2 \rangle = 0{\cdot}90$, and (*c*) $\langle T^* \rangle = 0{\cdot}47$, $\langle P_2 \rangle = 0{\cdot}99$.

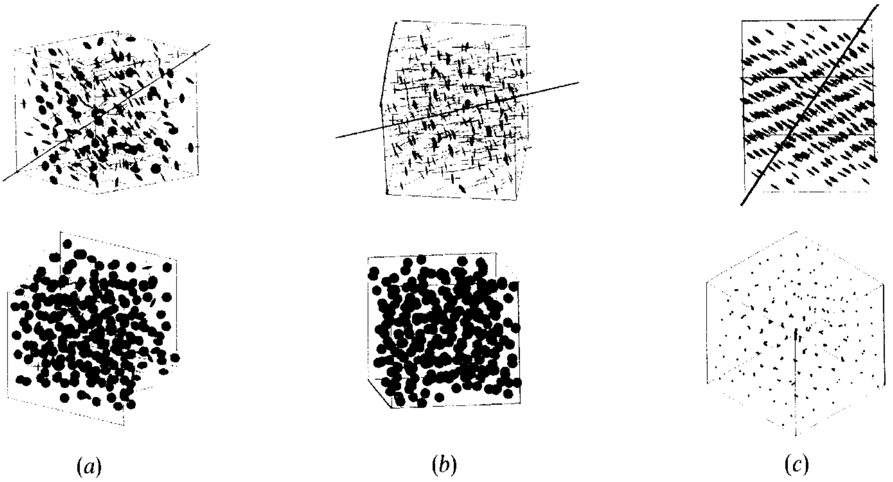

Figure 6. Three pairs of snapshots from typical configurations at instantaneous values of the order parameter $\langle P_2 \rangle$ of (*a*) 0·67, (*b*) 0·91 and (*c*) 0·99. The thick line in the box represents the direction of the director of the phase. The second snapshot is shown looking down the director for (*a*) and (*b*). In (*c*) the second snapshot shows the centres of mass of the molecules orthogonal to the column axes.

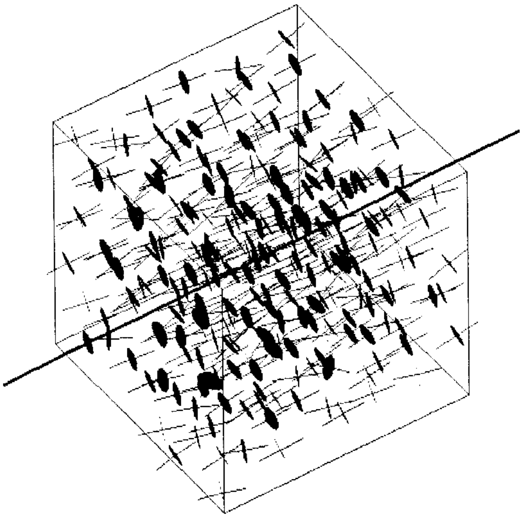

Figure 7. An enlarged snapshot of the configuration in figure 6 (*b*) at an instantaneous value of the order parameter $\langle P_2 \rangle$ of 0·91, exhibiting examples of short stacks of discs.

Figures 5 (*a*) and (*b*) show the radial distribution function together with transverse and longitudinal correlation functions at temperatures of $\langle T^* \rangle = 5{\cdot}0$ and $\langle T^* \rangle = 2{\cdot}77$, respectively. Figure 5 (*a*) demonstrates that there is no discernible change from liquid-like structure as the phase changes from isotropic to discotic nematic, but figure 5 (*b*) exhibits a one-dimensional density oscillation parallel to the director, consistent with the molecules being arranged in columns or layers with a separation $r^* = 0{\cdot}96$, coincident with the energy minimum in the pair potential. At the same temperatures, the transverse pair correlation function also begins to indicate the presence of structure with peaks occurring that become much more enhanced in the crystal phase as shown in figure 5 (*c*) at a reduced temperature of $\langle T^* \rangle = 0{\cdot}47$.

The second rank orientational correlation function, $G_2(r^*)$, exhibited a peak close to a reduced separation $r^*=0{\cdot}7$ in all cases. In the isotropic phase, $G_2(r^*)$ quickly decayed to a limiting value close to zero, indicating the absence of any long range order. In the nematic and higher order phases, $G_2(r^*)$ attains a limiting value of approximately $\langle P_2\rangle^2$ indicative of the persistence of orientational order at long range in these phases.

Figure 6 represents 'snapshots' of sample configurations taken during production runs at reduced temperatures of $\langle T^*\rangle=5{\cdot}0$, $\langle T^*\rangle=2{\cdot}8$ and $\langle T^*\rangle=0{\cdot}47$ corresponding to instantaneous values of the order parameter $\langle P_2\rangle=0{\cdot}67$, $\langle P_2\rangle=0{\cdot}91$ and $\langle P_2\rangle=0{\cdot}99$. In each case, two views of the same configuration are presented parallel and perpendicular to the director. Figure 6 (*a*) illustrates the discotic nematic phase. In figure 6 (*b*) we present two views of the higher order phase. Although these snapshots do not appear to exhibit a full discotic columnar phase, there is evidence of short stacks of discs as shown in figure 7. This short range columnar order is supported by the density oscillation in the longitudinal distribution function parallel to the director. Frenkel [1], in simulations of cut spheres, observed highly ordered short range stacks, but in this case the oscillations in the longitudinal distribution function died away within the simulation box. It is interesting to note that in figure 6 (*c*) and to a lesser extent in figure 6 (*b*), the molecules appear tilted within the columns. A similar effect was observed in the liquid crystal phase diagram of the Gay–Berne fluid [10] as a smectic B phase was compressed. Finally figure 6 (*c*) shows a crystal phase. The crystal shows a honeycomb structure with hexagonal symmetry, but not close packing. Other simulations of discotics using the Gay–Berne potential have yielded a final crystal with rectangular symmetry [11].

4. Conclusion

We have used molecular dynamics to simulate a system of discs interacting by a modified Luckhurst–Romano potential scaled by part of the well depth anisotropy term of the Gay–Berne potential. We have identified a phase transition from an isotropic liquid to a discotic nematic at a reduced temperature of $\langle T^*\rangle\approx 5{\cdot}5$. The discotic nematic phase is stable over a range of about three reduced temperature units, subsequently undergoing a further transition to a higher ordered phase at $\langle T^*\rangle\approx 2{\cdot}7$. The higher order phase is observed over a small reduced temperature range, with a transition to a crystal phase possessing hexagonal symmetry at $\langle T^*\rangle\approx 2{\cdot}6$. These results are similar to those of Emerson [11] for the Gay–Berne potential which provisionally identified nematic discotic and columnar discotic phase transitions at reduced temperatures of $\langle T^*\rangle\approx 11{\cdot}0$ and $\langle T^*\rangle\approx 4{\cdot}0$ respectively, at a reduced density of $\rho^*=3{\cdot}0$, the Gay–Berne crystal showing rectangular symmetry. The reduced CPU time required for the modified potential (5) will allow multi-site versions of the potential with differing geometries to be used to simulate discotic liquid crystals more realistically, allowing investigation of the effect of variable bond lengths, and more direct comparison with the Gay–Berne fluid.

We wish to acknowledge the award of a research studentship to MDD from the Science and Engineering Research Council (RS Quota Award ref. No. 9031742X0), plus a grant of CPU time on the Manchester Computing Centre Amdahl VP1200 vector processor (Award ref. GR/H55994).

References

[1] Veerman, J. A. C., and Frenkel, D., 1992, *Phys. Rev.* A, **45**, 5632.
[2] Azzouz, H., Caillo, J. M., Levesque, D., and Weis, J. J., 1992, *J. chem. Phys.*, **96**, 4551.

[3] Frenkel, D., Mulder, B. M., and McTague, J. P., 1985, *Molec. Crystals liq. Crystals*, **123**, 119.

[4] Luckhurst, G. R., and Romano, S., 1980, *Proc. R. Soc.* A, **373**, 111.

[5] Everitt, D. R. R., and Care, C. M., 1990, *Molec. Simul.*, **5**, 167.

[6] Berne, B. J., and Pechukas, 1972, *J. chem. Phys.*, **56**, 4213.

[7] Gay, J. G., and Berne, B. J., 1981, *J. chem. Phys.*, **74**, 3316.

[8] Adams, D. J., Luckhurst, G. R., and Phippen, R. W., 1987, *Molec. Phys.*, **61**, 1575.

[9] Luckhurst, G. R., Stephens, R. A., and Phippen, R. W., 1990, *Liq. Crystals*, **8**, 451.

[10] de Miguel, E., Rull, L. F., Chalam, M. K., and Gubbins, K. E., 1991, *Molec. Phys.*, **74**, 405.

[11] Emerson, A. P. J., 1991, Ph.D. thesis, University of Southampton, UK.

[12] Neal, M. P., De Luca, M. D., and Care, C. M., 1991, Poster presented at the NATO Advanced Workshop, Il Ciocco, Italy.

[13] Hockney, R. W., 1970, *Meth. comput. Phys.*, **9**, 136.

[14] Allen, M. P., and Tildesley, D. J., 1987, *Computer Simulation of Liquids* (Clarendon Press).

[15] Fincham, D., 1984, *CCP5 Quart.*, **12**, 47.

[16] Zannoni, C., 1979, *The Molecular Physics of Liquid Crystals*, edited by G. R. Luckhurst and G. W. Gray (Academic Press), Chap. 9, p. 191.

[17] Tildesley, D. J., 1984, *Molecular Liquids, Dynamics and Interactions*, edited by A. J. Barnes, W. J. Orville-Thomas and J. Yarwood (Reidel), (NATO ASI Series, Vol. 135) p. 519.